Insights into the Anticancer Activity of Chiral Alkylidene-β-Lactams and Alkylidene-γ-Lactams: Synthesis and Biological Investigation

Américo J. S. Alves,[a] Nuno G. Alves,[a] Mafalda Laranjo,[b,c,d] Clara S. B. Gomes,[e,f,g] Ana Cristina Gonçalves,[b,c,d,h] Ana Bela Sarmento-Ribeiro,[b,c,d,h] M. Filomena Botelho[b,c,d] and Teresa M. V. D. Pinho e Melo[a*]

[a] University of Coimbra, Coimbra Chemistry Centre-Institute of Molecular Sciences and Department of Chemistry, 3004-535 Coimbra, Portugal.

[b] Institute of Biophysics and Institute for Clinical and Biomedical Research (iCBR), Area of Environment Genetics and Oncobiology (CIMAGO), Faculty of Medicine, University of Coimbra, 3000-548 Coimbra, Portugal.

[c] Center for Innovative Biomedicine and Biotechnology (CIBB), University of Coimbra, 3000-548 Coimbra, Portugal.

[d] Clinical and Academic Centre of Coimbra, 3000-548 Coimbra, Portugal.

[e] LAQV-REQUIMTE, Department of Chemistry, NOVA School of Science and Technology, Universidade Nova de Lisboa, 2829-516 Caparica, Portugal;

[f] Associate Laboratory i4 HB-Institute for Health and Bioeconomy, School of Science and Technology,NOVA University Lisbon, 2819-516 Caparica, Portugal;

[g] UCIBIO-Applied Molecular Biosciences Unit, Department of Chemistry, School of Science and Technology, NOVA University Lisbon, 2819-516 Caparica, Portugal;

[h] Laboratory of Oncobiology and Hematology, Faculty of Medicine, University of Coimbra, 3000-548 Coimbra, Portugal.

**tmelo@ci.uc.pt*

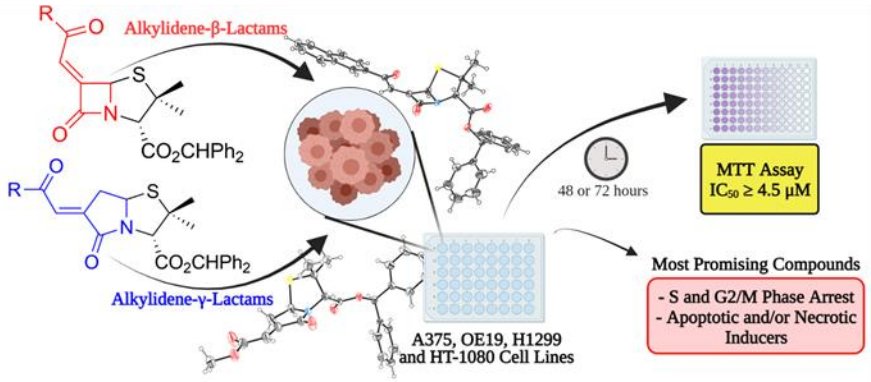

Abstract – Chiral alkylidene-β-lactams and alkylidene-γ-lactams were synthesized and screened for their *in vitro* activity against four human cancer cell lines (melanoma, esophageal, lung and fibrosarcoma carcinoma). Alkylidene-β-lactams were synthesized via Wittig reaction of diverse phosphorus ylides with benzhydryl 6-oxopenicillanate, derived from 6-aminopenicillanic acid. Moreover, novel chiral alkylidene-γ-lactams were synthesized through a multistep strategy starting from a chiral substrate (D-penicillamine). The *in vitro* assays allowed the identification of four compounds with IC_{50} values < 10 μM for A375 cell line, and three compounds with IC_{50} values < 10 μM for OE19 cell line. The effect of the most promising compounds on cell death mechanism, reactive oxygen species generation as well as the evaluation of their ability to act as MMP-9 inhibitors were studied. The reported results unveil the potential of alkylidene-β-lactams as anticancer agents.

Keywords: Alkylidene-β-lactam; Alkylidene-γ-lactam; Penicillanates; Anticancer Agents; Melanoma; Esophageal Cancer; Lung Cancer; Fibrosarcoma

1. Introduction

Cancer is one of the leading causes of death being responsible for nearly 10 million deaths annually and remains as one of the most difficult diseases to treat.[1] The rapid development of drug-resistant cancers, and the low specificity of some anticancer agents with the associated side effects are some of the major obstacles to overcome.[2] Thus, a major challenge of medicinal chemists around the world is the development of novel anticancer agents.

The β-lactam ring is the core structure of a wide range of successful antibiotics. The discovery of Penicillin G by Fleming had a huge impact on medicine, and since then researchers were inspired and turned their attention to the study of β-lactams. Although the major area of research on β-lactams has focused on antibacterial activity, since the beginning of 21th century a wide range of new pharmacologically active β-lactamic compounds were discovered displaying a range of other biological activities (*e.g.* antifungal, antiviral, anti-inflammatory, tryptase inhibitors).[3] Furthermore, there are also several examples where the β-lactam ring is associated with anticancer activity (Figure 1).[4]

Alkylidene-β-lactams are a class of attractive β-lactam derivatives that can be used as a scaffold for a wide range of synthetic transformations by exploring the reactivity of the C-C double bond (*e.g.* cycloaddition reactions, olefin metathesis, Michael additions).[5] Moreover, it was reported that alkylidene-β-lactams may act as enzymatic inhibitors [*e.g.* human leukocyte elastase, $IC_{50} \geq 0.5$ μM; matrix metalloproteinases (MMPs), $IC_{50} \geq 4$ μM; β-lactamase $IC_{50} \geq 5$ nM] and some derivatives show antioxidant properties.[6] Interestingly, Veinberg *et al.* demonstrated that alkylidene-β-lactams can also exhibit cytotoxic activity against some human and mouse tumor cell lines, namely HT-1080, MG-22A, B16 and Neuro 2A cell lines with IC_{50} values as low as 0.9 μM.[7] The alkylidene-γ-lactam ring is also in the core of natural and synthetic compounds showing biological properties such as anticancer (with IC_{50} values ≥ 20 μM in a wide range of cell lines) or analgesic activity (Figure 1).[8]

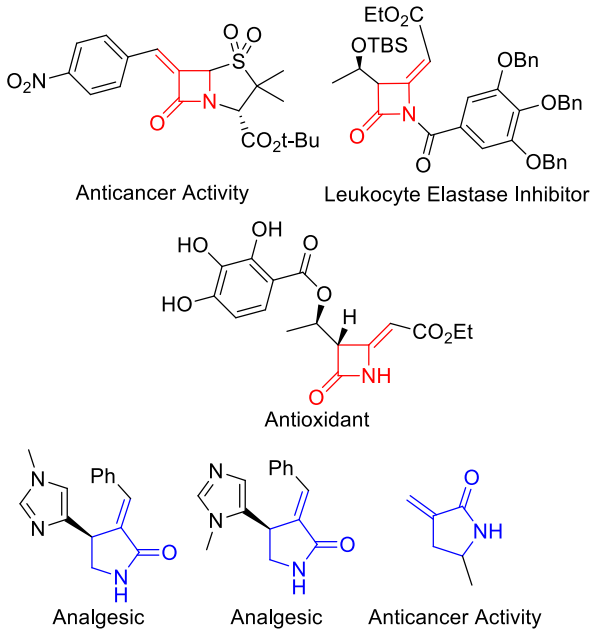

Figure 1. Representative examples of biologically active alkylidene-lactams

Herein, studies to unveil the bioactivity behavior of alkylidene-lactams as anticancer agents are described (Figure 2). The construction of a library alkylidene-β-lactams and alkylidene-γ-lactams was carried, designed to allow conclusions to be drawn regarding structure-activity relationships (SAR). The synthesized alkylidene-lactams were assayed for their *in vitro* cytotoxicity against four tumor cell lines. Moreover, further studies were carried out with the more promising derivatives in order to get an insight into the induced cell death mechanism.

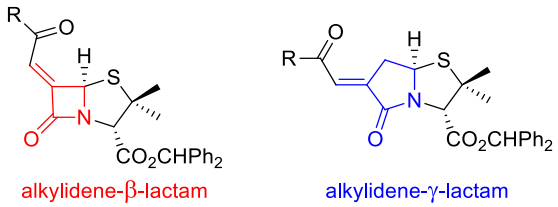

Figure 2. General molecular structure of alkylidene-β-lactams and alkylidene-γ-lactams.

2. Results and Discussion

2.1. Synthesis

To assess the activity of alkylidene-β-lactams as anticancer agents, a library of 14 6-alkylidene-penicillanates **1a-m** were synthesized by a known procedure, having 6-aminopenicillanic acid (6-APA) as starting material, a well-known raw material used for the synthesis of compounds containing the penicillanic core (Figure 3).[5b, c]

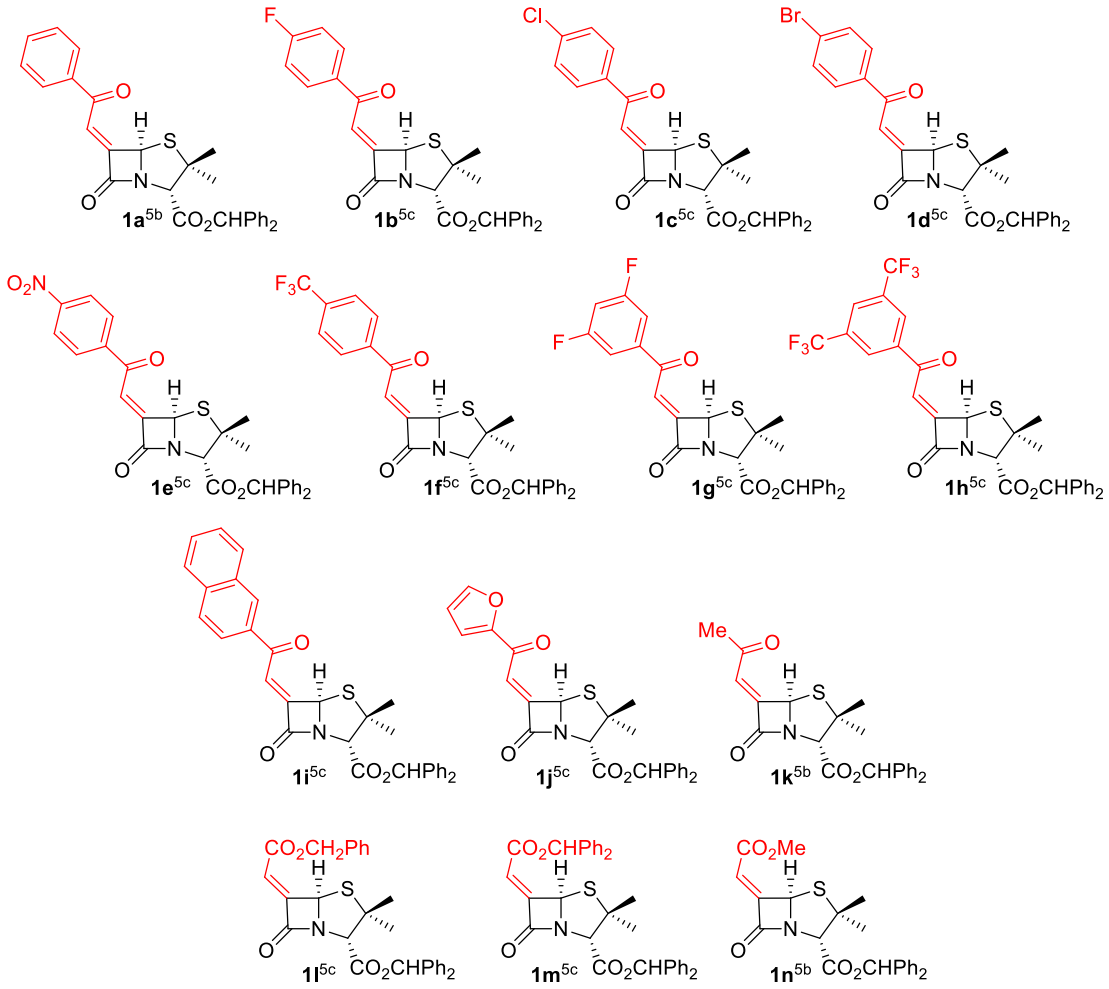

Figure 3. Library of synthesized alkylidene-β-lactams.

The strategy for the synthesis of these compounds containing the penicillanic core involves the synthesis of diazo-β-lactam **3** from benzhydryl 6-β-aminopenicillanate hydrochloride salt **2**,[9] followed by a rhodium catalyzed oxidation of the diazo derivative in the presence of propylene oxide to give oxo-β-lactam **4**.[10] The Wittig reaction of oxo-β-lactam **4** with the appropriate phosphorus ylide **5** affords the target alkylidene-β-lactams **1**. The synthesis of the novel alkylidene-β-lactam **1o**, containing an ethyl ester substituent at the carbon-carbon double bond, was achieved following this synthetic strategy in 36% overall yield (Scheme 1).

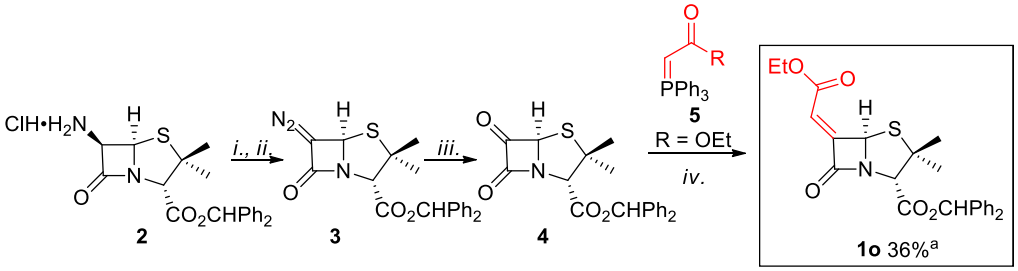

i. $NaHCO_3$ (sat. aq. sol.)/DCM;
ii. Isoamyl nitrite, TFA, EtOAc, 1 h, rt;
iii. Propylene oxide, $Rh_2(OAc)_4$, toluene, 15 min, 25-35 °C;
iv. Phosphorus ylide, DCM, 15 min (-55 °C), then rt.
[a] Overall yield from compound **2**

Scheme 1. Synthesis of benzhydryl (*Z*)-6-(ethoxycarbonylmethylidene)penicillinate (**1o**).

The molecular structure of alkylidene-β-lactam **1i** was determined by single-crystal X-ray diffraction, with its molecular structure represented in Figure 4 as an ORTEP3 diagram, and the most relevant bond lengths (Å) and angles (º) reported in the corresponding Figure caption. Compound **1i** crystallized as colorless plates, in the orthorhombic system, $P2_12_12_1$ space group, with one molecule in the symmetric unit. The dihedral angle between the two fused rings in the β-lactam is 48.6(3) º. The geometry of the carbon-carbon double bond C6–C24 was also established, unambiguously showing a *Z* conformation. The absolute structure was determined by a Flack analysis (943 Friedel pairs, η=0.06(8)) that assigns the *S,R* configuration to the chiral centers C3 and C5, respectively.

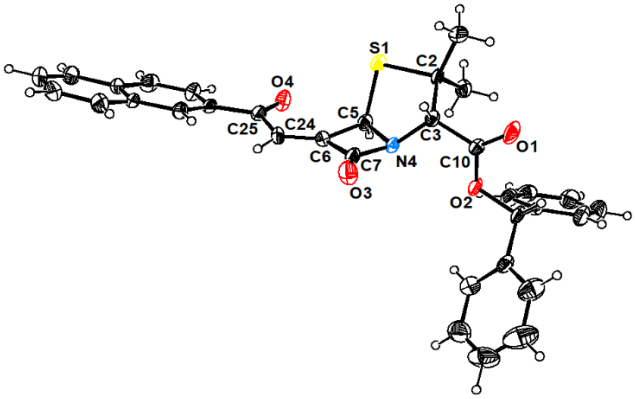

Figure 4. ORTEP representation of compound **1i**, using 30% level ellipsoids. Selected bond lengths: S1–C2 1.847(5) Å, C2–C3 1.562(7) Å, C3–N4 1.469(6) Å, N4–C7 1.408(7) Å, N4–C5 1.484(6) Å, C5–C6 1.508(8) Å, C6–C7 1.498(8) Å, C7–O3 1.192(7) Å, S1–C5 1.811(6) Å. Selected bond angles: C5–S1–C2 90.3(3)º, C5–N4–C7 93.0(4)º, C7–N4–C3 122.7(5)º, N4–C5–C6 87.3(4)º.

Previously studies on the anticancer activity of alkylidene-penicillanates have shown that the oxidation to the corresponding sulfoxide and sulfone derivatives can lead to increased biological activity.[7b] In this context, sulfoxides **6** and sulfones **7** were prepared from the corresponding alkylidene-penicillanates **1a,e** (Table 1). Carrying out the oxidation of alkylidene **1a** with 3 equivalents of *m*-CPBA for 30 minutes (entry 1) the corresponding sulfoxide **6a** was obtained as major product in 75% yield, along with sulfone **7a** (20% yield). By increasing the reaction time to 17 or 24 hours (entries 2 and 3) sulfone **7a** becomes the major product (56-63% yield) with sulfoxide **6a** isolated in moderate yield (21-29%). Treatment of alkylidene **1e** with *m*-CPBA for 17 h also led to the desired oxidation products **6b** and **7b** in 77% overall yield (29% and 48%, respectively, entry 4). In this specific case, increasing the reaction time to 24 hours did not lead to an improvement of the isolated yields (entry 5).

Table 1. *m*-CPBA oxidation of alkylidene-penicillanates leading to sulfoxide and sulfone derivatives.

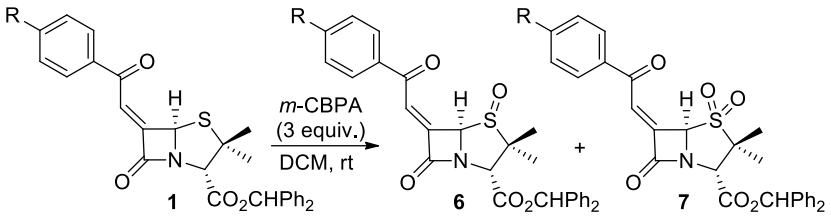

Entry	**1**, R	Reaction time	Products, Isolated yields
1	**1a**, 4-H	0.5 h	**6a** 75%, **7a** 20%
2	**1a**, 4-H	17 h	**6a** 27%, **7a** 56%
3	**1a**, 4-H	24 h	**6a** 21%, **7a** 63%
4	**1e**, 4-NO_2	17 h	**6b** 29%, **7b** 48%
5	**1e**, 4-NO_2	24 h	**6b** 21%, **7b** 37%

In order to evaluate if the β-lactam ring is a pharmacophoric feature associated with the anticancer activity, alkylidene-γ-lactams corresponding to the replacement of the four-membered β-lactam ring of 6-alkylidenepenicillanates **1a**,**1k** and **1n** by a five-membered γ-lactam ring were synthesized. Hence, having in mind the synthesis of alkylidene-γ-lactams **12**, we followed a multistep strategy starting from *D*-penicillamine and an L-aspartic acid derived aldehyde, previously developed by our research group, leading to compound **8**.[11] Amino-γ-lactam **9** was obtained by the neutralization reaction of the corresponding tosylate salt **8**. Subsequent treatment of **9** with sodium nitrite and perchloric acid at 0 ºC, allowed the synthesis of the diazo-γ-lactam **10** which was converted into the corresponding oxo-γ-lactam **11** as outlined in Scheme 2. Finally, the novel chiral alkylidene-γ-lactams **12a-c** were obtained via a Wittig reaction of oxo-γ-lactam **11** with the appropriate phosphorus ylide in moderate overall yields, ranging from 16% to 28% (from **8**).

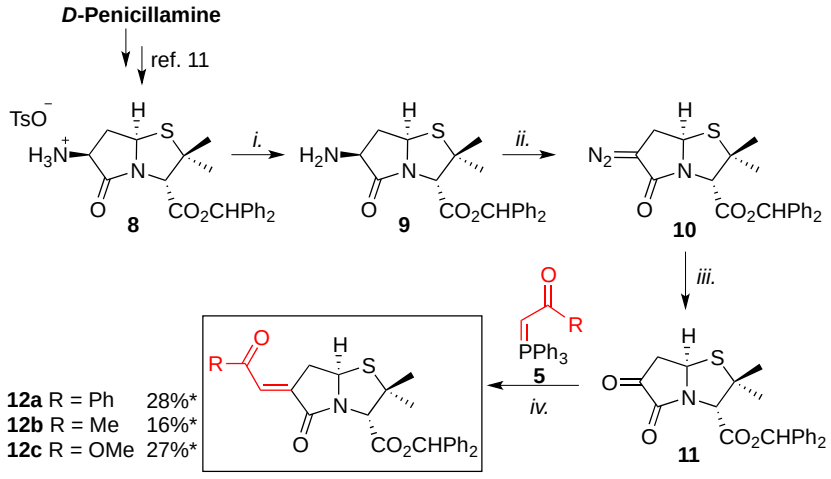

i. $NaHCO_3$ (sat. aq. sol.)/DCM, 30 min, rt;
ii. $NaNO_2$, $HClO_4$, DCM/H_2O, 1 h, 0 ˚C;
iii. Propylene oxide, $Rh_2(OAc)_4$, toluene, 15 min, 25-35 ˚C;
iv. Phosphorus ylide, DCM, 15 min (-55 ˚C), then rt.
from **8*

Scheme 2. Synthesis of chiral alkylidene-γ-lactams derived from *D*-penicillamine.

Knowledge about the three-dimensional conformation of alkylidene-γ-lactams **12** is important to determine if this class of compounds share similarity with their β-lactam analogues, namely the butterfly-like structure of the penicillanate core. Hence, the molecular structure of these interesting chiral alkylidene-γ-lactams, namely alkylidene **12c** was unambiguously established by single-crystal X-ray diffraction. Figure 5 depicts its ORTEP diagram, the most relevant bond distances (Å) and angles (º) being reported in the corresponding Figure caption. This derivative crystallized as colorless prisms in the orthorhombic system within the $P2_12_12_1$ space group, showing one molecule per asymmetric unit. Its molecular structure consists of an oxohexahydropyrrolo[2,1-*b*]thiazole derivative, with a dihedral angle between the two fused rings of 55.7(2) º. The absolute structure was determined by a Flack analysis (803 Friedel pairs, η=0.10(10)) that unambiguously assigns the *S,R* configuration to the chiral centers C3 and C7a, respectively. All distances and angles are within the expected values for similar compounds.[12] This study allowed also to establish the geometry of the carbon-carbon double bond.

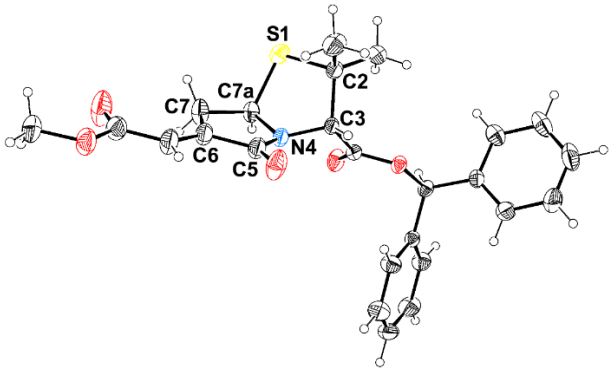

Figure 5. ORTEP representation of compound **12c**, using 30% level ellipsoids. Selected bond lengths: S1–C2 1.822(5) Å, C2–C3 1.558(6) Å, C3–N4 1.437(5) Å, N4–C7a 1.434(5) Å, N4–C5 1.354(5) Å, C5–C6 1.481(7) Å, C6–C7 1.478(6) Å, C7–C7a 1.520(6) Å, S1–C7a 1.820(5) Å. Selected bond angles: C7a–S1–C2 94.8(2)º, C5–N4–C7a 114.1(4)º, C7a–N4–C3 114.6(3)º, N4–C5–C6 106.7(4)º.

2.2. Cell Biology

2.2.1. Anticancer activity

In vitro studies regarding the anticancer activity of 6-(benzoylmethylene)penicillanates **1a-h**, **6**, **7** have been carried out against melanoma (A375) and esophageal (OE19) cancer human cell lines. The comparison of the activity of the compounds was made by analyzing the corresponding IC_{50} values calculated from the dose-response curves allowing SAR rationalization (Table 2). Alkylidene-β-lactam **1a** containing an unsubstituted benzoyl moiety showed moderated activity against A375 cell line (IC_{50} = 22.8 μM), and good activity against OE19 cell line (IC_{50} = 12.8 μM). The introduction of weak electron withdrawing groups (R = F, Cl, Br) at phenyl group *para*-position was also evaluated. In comparison with unsubstituted derivative **1a**, compound **1b** (R = 4-F) was the only one showing lower IC_{50} values against both cell lines (17.8 μM

and 12.1 μM, for A375 and OE19 cell lines, respectively). Strong electron withdrawing groups (R = CF_3, NO_2) at *para*-position of the phenyl group led to a decrease in cytotoxicity, which was more pronounced for the nitro derivative (**1e**, IC_{50} = 50.3 μM and 44.1 μM, for A375 and OE19 cell lines, respectively). Interestingly, disubstituted 3,5-difluoro derivative **1g** presented IC_{50} values similar to those obtained for the unsubstituted benzoyl (**1a**) or 4-fluorophenyl (**1b**) derivatives in A375 cell line, while the derivative containing two CF_3 groups at *meta*-positions (**1h**) showed poor activity. Sulfoxide **6b** and both sulfones **7a** and **7b** showed also poor cytotoxic against both cell lines. However, we were pleased to observe that sulfoxide **6a**, derived from alkylidene-β-lactam **1a**, proved to be very active against A375 melanoma cell line (IC_{50} = 4.5 μM).

In vitro studies were extended to the screening of selected 6-(benzoylmethylene)penicillanates using a longer incubation time (72 h, see Table S1). No significant differences were observed, compared to the 48 h assays, in the case of A375 cell line. However, at 72 h the cytotoxic effect was higher for OE19 cell line than at 48 h for both tested compounds (**1a**, IC_{50} = 8.6 μM; **1b**, IC_{50} = 10.7 μM).

Table 2. IC_{50} values and respective confidence intervals at 95% (CI_{95}) of 6-(benzoylmethylene)penicillanate derivatives **1a-h**, **6**, **7** and cisplatin in melanoma (A375) and esophageal (OE19) cell lines. Values were determined by dose-response sigmoidal fitting. Each experiment was performed in triplicate and repeated in at least two independent experiments (n ≥ 2).

Compound	A375 (48 h)		OE19 (48 h)	
	IC_{50} (μM)	CI_{95}	IC_{50} (μM)	CI_{95}
1a	22.8	[18.1;28.7]	12.8	[10.5;15.6]
1b	17.8	[13.6;23.3]	12.1	[10.7;13.6]
1c	48.6	[very wide]	14.6	[10.1;21.1]
1d	29.7	[23.3;38.0]	13.8	[11.3;16.8]
1e	50.3	[32.8;77.3]	44.1	[29.2;66.8]
1f	26.7	[19.2;37.2]	15.6	[11.4;22.1]
1g	19.1	[17.7;20.5]	17.6	[13.6;22.8]
1h	39.2	[26.3;58.5]	48.5	[very wide]
6a	4.5	[4.2;4.9]	23.7	[15.9;35.3]
6b	48.2	[27.6;84.2]	92.4	[very wide]
7a	17.5	[12.0;25.4]	53.1	[33.4;84.4]
7b	76.7	[37.7;156.2]	95.5	[very wide]
Cisplatin	8.4	[7.4;9.5]	96.3	[85.8; 108.2]

In order to get further details regarding structure-activity relationships, we examined the activity of 6-alkylidenepenicillanates bearing 2-naphthoyl (**1i**), 2-furoyl (**1h**) and acetyl (**1k**) substituents as well as ester groups (**1l-o**) (Table 3). It was observed that the replacement of the benzoyl group of **1a** by substituents incorporating other aromatic systems, namely naphthoyl and furoyl groups, or the replacement by an acetyl group led to cytotoxicity decrease. Particularly interesting results were observed in the study of alkylidene-β-lactams containing an ester moiety at the carbon-carbon double bond. Despite the moderate activity of the methyl ester derivative (**1n**) against A375 and OE19 cell lines, the alkylidene-β-lactam **1l** substituted with a benzyl ester and the newly synthesized ethyl ester derivative **1o** showed low IC_{50} values against both cell lines (**1l**: 7.1 μM and 8.2 μM and **1o**: 7.0 μM and 11.2 μM for A375 and OE19 cell lines, respectively). Additionally, benzhydryl ester derivative showed good activity against the

melanoma A375 cell line (IC_{50} = 9.1 μM) but was slightly less of active than benzyl ester alkylidene-β-lactam **1l**, indicating that the introduction of a second phenyl group in the ester moiety impairs its biological activity.

The anticancer assays performed with 72 h of incubation time for this set of compounds led only to better results in OE19 cell line (Table S2) as previously observed for the previous studied 6-alkylidenepenicillanates (see Table S1). It is important to highlight the low IC_{50} values observed for compounds **1l** and **1o** (IC_{50} = 4.6 μM and 5.3 μM, respectively) against this cell line.

Table 3. IC_{50} values and respective CI_{95} of compounds **1i-o** and cisplatin in melanoma (A375) and esophageal (OE19) cell lines. Values were determined by dose-response sigmoidal fitting. Each experiment was performed in triplicate and repeated in at least two independent experiments (n ≥ 2).

Compound	A375 (48 h)		OE19 (48 h)	
	IC_{50} (μM)	CI_{95}	IC_{50} (μM)	CI_{95}
1i	36.5	[20.2;65.9]	19.5	[14.2;26.9]
1j	26.0	[18.0;37.6]	54.3	[36.3;81.1]
1k	63.0	[45.0;88.1]	51.9	[34.0;79.1]
1l	7.1	[6.6;7.7]	8.2	[6.7;10.0]
1m	9.1	[6.4;12.8]	21.6	[16.0;29.3]
1n	24.6	[17.6;34.3]	20.2	[14.7;27.6]
1o	7.0	[5.9;8.4]	11.2	[9.8;12.7]
Cisplatin	8.4	[7.4;9.5]	96.3	[85.8; 108.2]

Despite a highly structural similarity to the β-lactam analogues, as confirmed by the X-ray diffraction study (see Figures 4 and 5), the novel alkylidene-γ-lactams **12** did not show any cytotoxic activity against both A375 and OE19 cell lines, with higher IC_{50} values (Table 4). These results confirm the important role of the β-lactam nucleus in the anticancer activity.

Table 4. IC_{50} values and respective CI_{95} of compounds **12** in melanoma (A375) and esophageal (OE19) cell lines. Values were determined by dose-response sigmoidal fitting. Each experiment was performed in triplicate and repeated in at least two independent experiments (n ≥ 2).

Compound	A375 (48 h)		OE19 (48 h)	
	IC_{50} (μM)	CI_{95}	IC_{50} (μM)	CI_{95}
12a	>100	----	73.3	[42.2;127.3]
12b	>100	----	>100	----
12c	>100	----	99.7	[very wide]

Next, we broadened our anticancer studies to HT-1080 (fibrosarcoma cell line) and H1299 (human lung cancer cell line) cell lines, screening a selection of 6-alkylidenepenicillanates having different chemical moieties (Table 5). The most active compounds against A375 and OE19 were also the most active against HT-1080 and H1299 cell lines. However, the screening assays showed a lack of sensibility of these two cell lines against the tested compounds leading to higher IC_{50} values. Nevertheless, we should highlight the results obtained for compound **1l (**11.7 μM and 9.44 μM, for HT-1080 and H1299 cell lines, respectively). As observed in the previous assays, carrying

out the screening with 72 h of incubation did not lead to better results, with exception of compound **1o** in HT-1080 cell line (Table S3).

Table 5. IC_{50} values and respective CI_{95} of compounds **1a**,**b**, **1j-m**, **1o**, **6a**, **7a**, **12b** and cisplatin in HT-1080 and H1299 cell lines. Values were determined by dose-response sigmoidal fitting. Each experiment was performed in triplicate and repeated in at least two independent experiments ($n \geq 2$).

Compound	HT-1080 (48 h)		H1299 (48 h)	
	IC_{50} (μM)	CI_{95}	IC_{50} (μM)	CI_{95}
1a	21.1	[18.5;24.0]	39.0	[25.4;59.8]
1b	11.2	[9.9;12.6]	25.2	[20.0;31.6]
1j	45.5	[35.3;48.8]	61.5	[34.7;109.0]
1k	20.8	[18.3;23.5]	24.2	[18.2;32.1]
1l	11.7	[10.7;12.9]	9.4	[8.0;11.1]
1m	15.2	[13.3;17.4]	22.4	[17.5;28.8]
1o	25.1	[20.4;30.9]	15.0	[12.1;18.7]
6a	65.5	[36.4;117.8]	92.4	[very wide]
7a	19.5	[16.4;23.3]	50.1	[very wide]
12b	>100	----	>100	----
Cisplatin	16.3	[14.5;18.3]	69.1	[61.4;77.7]

2.2.2. Types of cell death and cell morphology

To further study the effect of the compounds on cell viability and the induced mechanism of cell death on A375 cells, flow cytometry studies were performed with compounds **1l**, **1m**, **1o** and **6a** in two concentrations (Figure 6). It was possible to conclude that regardless of the studied compound, the treatment with a concentration of 5 μM did not lead to considerable changes when compared to control cells. However, when cells were treated with 10 μM concentration major alterations on the induced mechanism of cell death were visible. Both compounds **1l** and **1o** induce a significant decreasing in the viable cells (**1l**: 56.25±4.65%; **1o**: 63.00±4.69%), an increasing in the late apoptosis/necrosis (**1l**: 13.00±0.82%; **1o**:11.50±2.65%) and in necrosis (**1l**: 24.00±6.68%; **1o**: 20.75±1.50%), comparing to control cells (V: 93.63±1.37%; LA/N: 1.83±0.41%; N: 1.17±0.41%). The same profile was observed for compound **1m** (V: 73.50±1.73%; LA/N: 7.75±1.89%; N: 14.75±2.87%) despite the lower values observed for apoptosis/necrosis and necrosis. On the other hand, compound **6a** (V: 89.17±3.37%; LA/N: 4.17±0.98%; N: 3.00±2.45%) did not show major alterations in comparison with control cells. This observation indicates that compound **6a** is reducing the metabolic activity of A375 cells without inducing apoptosis and/or necrosis. A plausible rationalization for this observation is that compound **6a** may induce the cells to enter in a state of quiescence, which is characterized for having a reduced metabolic activity but does not lead cells to apoptotic and/or necrotic stages.[13]

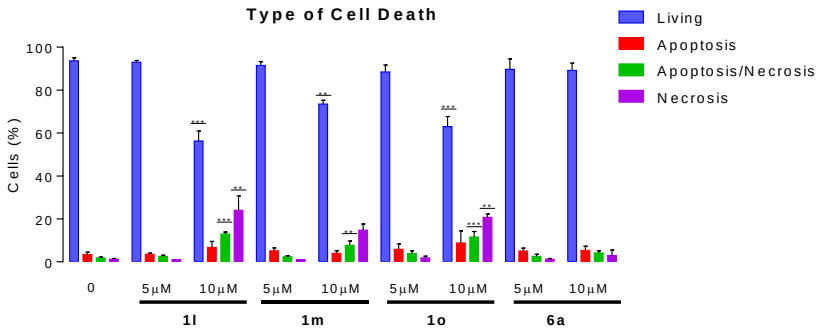

Figure 6. Viability and types of cell death induced by compounds **1l**, **1o**, **1m** and **6a** after 48 h of incubation in the human melanoma A375 cells, assessed by flow cytometry using dual staining with AV and PI. Results are presented as mean ± SD of viable cells (V), in initial apoptosis (IA), in late apoptosis and/or necrosis (LA/N) and in necrosis (N) of three independent experiments (n=3) performed in duplicate. Statistical significance: ∗p < 0.05; ∗∗p < 0.01, ∗∗∗p < 0.001.

Morphological evaluation of the control cells showed that they were homogeneous in size with an almost perfect circular shape (Figure 7). However, after the incubation with compound **1l** it was possible to observe either the formation of several blebs, a typical feature of apoptosis, or the loss of cell integrity.

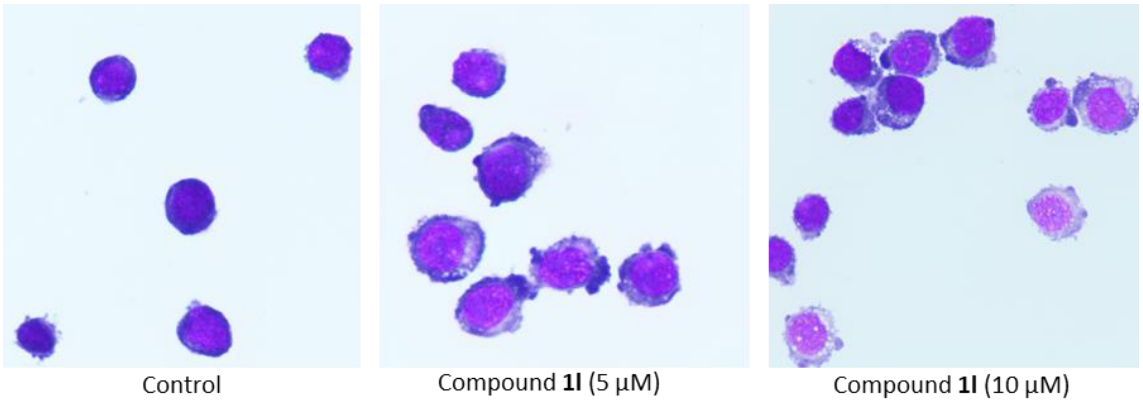

Figure 7. Morphological evaluation of A375 cells after May–Grünwald– Giemsa staining. The evaluation was performed in cells not submitted to treatment (control) and submitted to 5 or 10 µM of compound **1l** for 48 h. The images were randomly taken and are representative of each condition (50x).

2.2.3. Cell Cycle Analysis

Cell cycle analysis was conducted in A375 melanoma cell line for compounds **1l**, **1m**, **1o** and **6a** in two concentrations (5 and 10 µM) (Figure 8). Compound **1l** (5 µM), decreased the population of cells in the G1 phase (71.25±1.50%) with a significant increase of cells in S (19.50±1.73%) and G2/M (8.75±0.96%) phases, compared to control cells (G1: 83.50±1.87%; S:11.33±1.86%; G2/M: 5.17±0.75%). Moreover, changes were more pronounced when cells were treated with 10 µM of **1l** (G1 phase: 58.33±6.62%; S phase: 29.67±5.01%; G2/M phase: 12.00±1.79%). Compound **1o** led to similar results at 10 µM with a decrease cells' population in G1 phase (61.75±1.50%) and an increase of

cells in S (25.75±1.50%) and G2/M (12.50±0.58%) phases. Regarding compound **1m**, major changes in cell arrest were only observed when cells were treated with 10 μM concentration, leading to a decrease of cells in G1 phase (67.67±4.27%) which is linked with a slight increase of the population in S phase (15.33±2.07%) and a 2.5-fold increase in the percentage of cells in G2/M phase (13.00±2.68%).

In order to rationalize these results, it must be taken into account that the S phase is responsible for the synthesis and replication of DNA, and the G2/M phase is responsible for the synthesis of some proteins and mitosis. Thus, since compounds **1l**, **1m** and **1o** induce cell arrest in S and G2/M phases, they may act by interfering in the DNA or protein synthesis. Moreover, this hypothesis can also be supported by the presence of a Michael acceptor in the structure of our alkylidene-β-lactams. Finally, no significant changes were observed in the cell cycle profile for cells treated with compound **6a**. This means that compound **6a** induces a blockade in the G0/G1 phase, without any effect in the other phases of the cell cycle, corroborating the hypothesis that this compound induces a state of quiescence where cells stop dividing.[13]

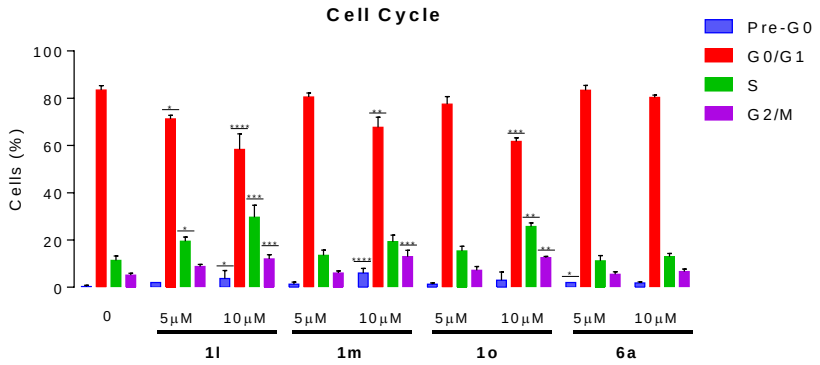

Figure 8. Cell cycle analysis after treatment with compounds **1l**, **1o**, **1m** and **6a** with 48 h of incubation in the human melanoma A375 cells, assessed by flow cytometry. Results are presented as mean ± SD of three independent experiments (n=3) performed in duplicate. Statistical significance: ∗p < 0.05; ∗∗p < 0.01, ∗∗∗p < 0.001, ∗∗∗∗p < 0.0001.

2.2.4. Reactive Oxygen Species

Considering the importance of intracellular reactive oxygen species (ROS) production as a mechanism of anticancer agents, the presence of intracellular peroxides and superoxide anion was assessed (Figure 9). It is possible to observe a decrease of intracellular peroxides, being more pronounced in the case of compound **1l**. This decrease could be explained by the activation of antioxidant pathways. Moreover, the reduction in peroxides production was also observed for compounds **1o** and **1m** (10 μM) with an incubation time of 48 h. On the other hand, with exception of a slight decrease observed for compound **1o** (5 μM with 48 h of incubation), no substantial changes were observed in the superoxide anion production profile when compared to control values.

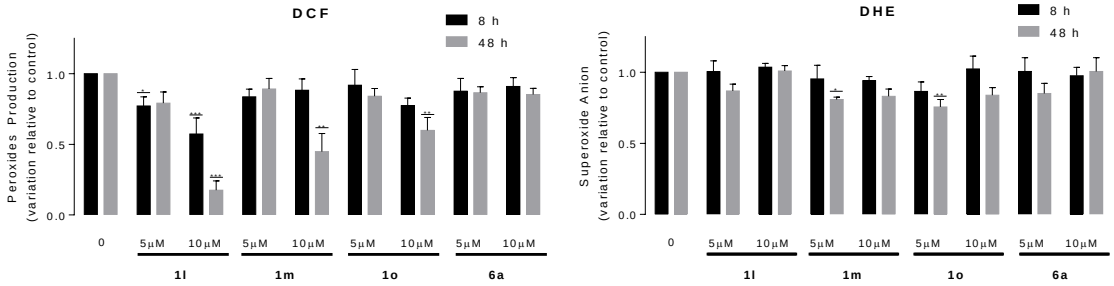

Figure 9. Intracellular production of ROS namely peroxides and superoxide anion, in the human melanoma A375 cells after treatment with compounds **1l**, **1o**, **1m** and **6a.** The analyses were carried out with 8 h or 48 h of incubation. Results are presented as mean ± SD of two independent experiments (n=2) performed in duplicate. Statistical significance: ∗p < 0.05; ∗∗p < 0.01; ∗∗∗p < 0.001.

2.2.5. Zymography

Matrix metalloproteinases (MMPs) are zinc-dependent endopeptidases responsible for tissue remodeling.[14] MMP-9 is one of the most studied and complex MMPs which belongs to gelatinase family. This MMP is responsible either for inhibiting or stimulating the extracellular matrix degradation process which is essential for tumor invasion or metastasis.[14b, 15] In this context, a set of 11 compounds were screened for their ability to inhibit MMP-9 (Figure 10). Thus, the gelatinolytic activity of MMP-9 secreted from fibrosarcoma cell line HT-1080 was evaluated with gelatin zymography. It was observed that the five compounds with moderate to good anticancer activity (*e.g.* **1a**, **1b**, **1l**, **1m** and **1o**), led to a slight reduction of the expression of MMP-9 when compared to control values. Interestingly, alkylidene-γ-lactams **12a** and **12c** proved to be the most efficient MMP-9 inhibitors (61.4±3.90% and 52.9±6.00%, when compared to control, respectively) among the studied compounds. The MMP-9 inhibitory effect observed for compounds **12a,c**, opens the way for further studies aiming at developing a new class of alkylidene-γ-lactams-based MMP-9 inhibitors to treat MMP-9 associated diseases such as cardiovascular diseases, lung diseases, arthritis, neurodegenerative diseases and central nervous system (CNS) disorders.[16]

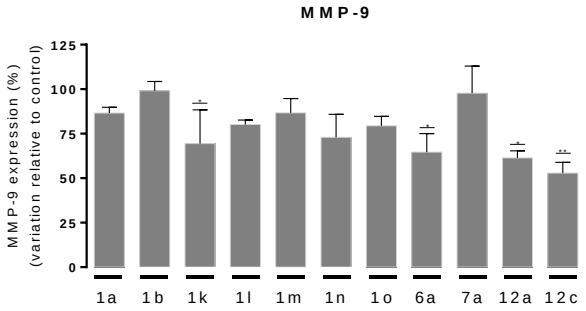

Figure 10. MMP-9 expression after treatment with a set of alkylidene-lactams at 10 µM. MMP-9 expression was evaluated by gelatin zymography. Results are presented as mean ± SD of at least three independent experiments (n≥3). Statistical significance: ∗p < 0.05; ∗∗p < 0.01.

3. Conclusion

Structural modulation of chiral α-alkylidene-substituted β-lactams and γ-lactams was carried out, leading to the synthesis of new chiral alkylidene-lactams. A synthetic route has been established for the synthesis of α-alkylidene-γ-lactams from D-penicillamine. *In vitro* studies regarding the anticancer activity of 6-aroylmethylene-, 6-acetylmethylene- and 6-alkoxycarbonylmethylene-penicillanates were carried out. Four compounds (**1l**, **1m**, **1o** and **6a**) with IC_{50} values below 10 μM in A375 human melanoma cells, and three compounds (**1l**, **1m**, **1o**) with IC_{50} values below 10 μM in OE19 human esophageal carcinoma cells stood out. Remarkably, compound **6a** showed an IC_{50} value of 4.5 μM against A375 cell line. Compound **1l** showed good activity on HT-1080 human fibrosarcoma, H1299 human lung cancer, and particularly against OE19 cell line (4.6 μM). Alkylidene-β-lactams induce cell apoptosis and necrosis and block the cell cycle in S and G2/M phases, while alkylidene-γ-lactams are potential MMP-9 inhibitors. The reported results show that the β-lactamic core together with the presence of an ester substituent are important structural features to ensure anticancer activity, a relevant SAR information for the design of further structural modulations aiming at the development of new and more potent drugs against cancer.

4. Experimental

4.1. Chemistry

General: Thin-layer chromatography (TLC) analyses were performed using precoated silica gel plates. Flash column chromatography was performed with silica gel 60 as the stationary phase. ^{1}H Nuclear magnetic resonance (NMR) spectra (400 MHz) and ^{13}C NMR spectra (100 MHz) were recorded in $CDCl_3$ as solvent. Chemical shifts are expressed in parts per million (ppm) relatively to internal tetramethylsilane (TMS) and coupling constants (*J*) are expressed in Hertz (Hz). Infrared spectra (IR) were recorded in a Fourier Transform spectrometer coupled with a diamond Attenuated Total Reflectance (ATR) sampling accessory. High-resolution mass spectra (HRMS) were obtained on a TOF VG Autospect M spectrometer with electrospray ionization (ESI) or on a Orbitrap q-Exactive Focus spectrometer coupled to a Vanquish HPLC with ESI. Melting points (mp) were determined in open glass capillaries. Optical rotations were measured on an Optical Activity AA-5 electrical polarimeter. 6-Alkylidenepenicillanates **1a-n**,[5b, c] and diazo-γ-lactam **10**[11] were prepared as described in the literature.

4.1.1. *Synthesis of benzhydryl 6-(Z)-(ethoxycarbonylmethylidene)penicillanate **1o***

A solution of 6-β-aminopenicillanate hydrochloride salt **2**[9] (1.00 g, 2.38 mmol) in dichloromethane (75 mL) was washed with a saturated aqueous solution of $NaHCO_3$ (2 x 75 mL), and the aqueous phase was extracted with dichloromethane (2 x 50 mL). The organic extracts were combined, dried and concentrated under reduced pressure to obtain the corresponding 6-β-aminopenicillanate. To a solution of 6-β-aminopenicillanate (2.38 mmol) in ethyl acetate (7 mL), isoamyl nitrite (1.2 equiv., 0.382 mL) was added followed by a catalytic amount of trifluoroacetic acid (two drops). The reaction mixture was stirred at room temperature for 1 h and concentrated under reduced pressure to obtain diazo-lactam **3** which was used, without further purification, in the synthesis of 6-

oxopenicillinate **4**. Rhodium acetate dimer (4×10^{-3} equiv., 9.5×10^{-3} mmol) was dissolved in toluene (9 mL) in a two-neck round bottom flask under inert atmosphere. Next, propylene oxide (99 equiv., 235.85 mmol, 16.3 mL) was added dropwise followed by a dropwise addition of a solution of the previously isolated diazo-lactam **3** in toluene (9 mL). The reaction was stirred for 15 min and concentrated under reduced pressure to give benzhydryl 6-oxopenicillinate **4**. Next, freshly synthesized benzhydryl 6-oxopenicillinate **4** was dissolved in dichloromethane (12 mL), the solution was cooled to –55 °C under nitrogen, and a solution of phosphorus ylide **5** (2.26 mmol) in dichloromethane (30 mL) was added dropwise. Stirring was continued for 15 min, then the solution was warmed to room temperature and washed with water (20 mL). The organic layer was separated, dried, and concentrated under reduced pressure. Purification of the crude product by flash chromatography (hexane/ethyl acetate, 4:1) gave compound **1o** as a white solid (373 mg, 0.857 mmol, 36% overall yield). mp 72.6–74.4 °C; $[\alpha]_D^{25}$ = + 280 (c 0.5 in CH_2Cl_2); IR (ATR) ν: 968, 1069, 1171, 1256, 1287, 1497, 1719, 1773 and 2984 cm^{-1}; ^1H NMR δ ($CDCl_3$): 1.28 (s, 3H), 1.33 (t, *J* = 7.1 Hz, 3H), 1.57 (s, 3H), 4.20-4.31 (m, 2H), 4.66 (s, 1H), 6.03 (d, *J* = 1.0 Hz, 1H), 6.29 (d, *J* = 1.1 Hz, 1H), 6.96 (s, 1H), 7.29-7.40 (m, 10H); ^{13}C NMR δ ($CDCl_3$): 14.3, 25.6, 33.9, 61.8, 64.0, 69.3, 70.8, 78.6, 116.1, 127.2, 127.7, 128.5, 128.7, 128.8, 139.2, 139.3, 156.6, 163.9, 166.5, 166.9; HRMS (ESI-TOF) m/z: $[M+Na]^+$ Calcd $C_{25}H_{25}NNaO_5S$ 474.1346, found 474.1340.

4.1.2. General procedure for the oxidation of 6-alkylidenepenicillanates

A mixture of the 6-alkylidenepenicillanate (0.100 g) and *m*-CPBA (3 equiv.) in dichloromethane (10 mL) was stirred at room temperature for the time indicated in each case (Method A: 0.5 h; Method B: 17 h; Method C: 24 h). Upon completion, the solution was washed twice with a 10% aqueous solution of Na_2SO_4 and the organic layer was extracted with dichloromethane. The combined organic extracts were dried, and the solvent evaporated off. The product was purified by flash chromatography.

*4.1.2.1. Benzhydryl 1-oxo-6-(Z)-(benzoylmethylidene)penicillanate **6a** and benzhydryl 1,1-dioxo-6-(Z)-(benzoylmethylidene)penicillanate **7a***

Prepared from 6-alkylidenepenicillanate **1a** (0.206 mmol, 0.100 g), as described in the general procedure. Purification of the crude product by flash chromatography (hexane/ethyl acetate, 2:1), gave, in order of elution, **7a** as a white solid (Method A: 21.3 mg, 0.041 mmol, 20%; Method B: 59.9 mg, 0.116 mmol, 56%; Method C: 67.3 mg, 0.131 mmol, 63%) and **6a** as a white solid (Method A: 77 mg, 0.154 mmol, 75%; Method B: 27.3 mg, 0.054 mmol, 27 %; Method C: 22 mg, 0.044 mmol, 21%).

6a: mp 71.7–73.7 °C; $[\alpha]_D^{25}$ = + 360 (c 0.25 in CH_2Cl_2); IR (ATR) ν: 976, 1107, 1051, 1155, 1232, 1349, 1448, 1595, 1635, 1702, 1747, 1780 and 2972 cm^{-1}; ^1H NMR δ ($CDCl_3$): 1.02 (s, 3H), 1.69 (s, 3H), 4.84 (s, 1H), 5.81 (d, *J* = 0.9 Hz, 1H), 7.02 (s, 1H), 7.32-7.41 (m, 10H), 7.53 (t, *J* = 7.7 Hz, 2H), 7.65 (d, *J* = 7.4 Hz, 1H), 7.67 (d, *J* = 1.3 Hz, 1H), 7.99-8.00 (m, 2H); ^{13}C NMR δ ($CDCl_3$): 18.3, 19.7, 66.8, 73.8, 78.9, 82.0, 119.8, 127.0, 127.9, 128.7, 128.8, 128.9, 129.0, 129.3, 140.0, 166.1, 167.4, 188.5; HRMS (ESI-TOF) m/z: $[M+Na]^+$ Calcd $C_{29}H_{25}NNaO_5S$ 522.1346, found 522.1340.

7a: mp 88.5–90.5 °C; $[\alpha]_D^{25}$ = + 270 (c 0.5 in CH_2Cl_2); IR (ATR) ν: 976, 1006, 1118, 1168, 1232, 1327, 1149, 1636, 1752, 1787 and 2934 cm^{-1}; ^1H NMR δ ($CDCl_3$): 1.21 (s, 3H), 1.61 (s, 3H), 4.61 (s, 1H), 5.60 (d, *J* = 0.9 Hz, 1H), 7.02 (s, 1H), 7.33-7.39 (m, 10H), 7.53 (t, *J* = 7.8 Hz, 2H), 7.66 (t, *J* = 7.4 Hz, 1H), 7.73 (d, *J* = 1.3 Hz, 1H), 8.02-8.04 (m,

2H); ^{13}C NMR δ ($CDCl_3$): 19.3, 19.9, 63.8, 64.6, 71.1, 79.2, 121.7, 126.9, 127.7, 128.4, 128.7, 128.8, 129.0, 129.1, 134.7, 136.1, 138.6, 138.8, 144.0, 166.0, 166.6, 187.1; HRMS (ESI-TOF) m/z: $[M+Na]^+$ Calcd $C_{29}H_{25}NNaO_6S$ 538.1295, found 538.1289.

*4.1.2.2. Benzhydryl 1-oxo-6-(Z)-(4-nitrobenzoylmethylidene)penicillanate **6b** and benzhydryl 1,1-dioxo-6-(Z)-(4-nitrobenzoylmethylidene)penicillanate **7b***

Prepared from 6-alkylidenepenicillanate **1e** (0.189 mmol, 0.100 g), as described in the general procedure. Purification of the crude product by flash chromatography (hexane/ethyl acetate, 2:1), gave, in order of elution, **7b** as a yellow solid (Method B: 55.9 mg, 0.0997 mmol, 48%; Method C: 39.3 mg, 0.070 mmol, 37%) and **6b** as a pale-yellow solido (Method B: 32.2 mg, 0.059 mmol, 29%; Method C: 22.2 mg, 0.040 mmol, 21 %).

6b: mp 83.7–85.7 °C; $[\alpha]_D^{25}$ = + 250 (c 0.5 in CH_2Cl_2); IR (ATR) ν: 1010, 1067, 1158, 1206, 1341, 1524, 1748, 1782 and 2929 cm^{-1}; ^{1}H NMR δ ($CDCl_3$): 1.03 (s, 3H), 1.70 (s, 3H), 4.85 (s, 1H), 5.81 (d, *J* = 0.7 Hz, 1H), 7.03 (s, 1H), 7.33-7.39 (m, 10H), 7.65 (d, *J* = 1.3 Hz, 1H), 8.16 (d, *J* = 8.9 Hz, 2H), 8.38 (d, *J* = 8.9 Hz, 2H); ^{13}C NMR δ ($CDCl_3$): 18.2, 19.7, 67.0, 74.0, 79.1, 82.0, 118.8, 124.4, 127.0, 127.9, 128.5, 128.8, 128.9, 130.0, 138.9, 139.2, 140.9, 149.1, 151.1, 165.4, 167.2, 187.2; HRMS (ESI-TOF) m/z: $[M+Na]^+$ Calcd $C_{29}H_{24}N_2NaO_7S$ 567.1196, found 567.1191.

7b: mp 94.4–96.4 °C; $[\alpha]_D^{25}$ = + 190 (c 0.5 in CH_2Cl_2); IR (ATR) ν: 1009, 1118, 1169, 1213, 1323, 1524, 1602, 1647, 1753, 1790 and 2931 cm^{-1}; ^{1}H NMR δ ($CDCl_3$): 1.21 (s, 3H), 1.62 (s, 3H), 4.63 (s, 1H), 5.59 (d, *J* = 0.9 Hz, 1H), 7.02 (s, 1H), 7.33-7.39 (m, 10H), 7.70 (d, *J* = 1.3 Hz, 1H), 8.19 (d, *J* = 8.9 Hz, 2H), 8.39 (d, *J* = 8.9 Hz, 2H); ^{13}C NMR δ ($CDCl_3$): 18.5, 20.0, 64.1, 64.9, 71.2, 79.5, 120.7, 124.5, 127.0, 127.8, 128.6, 128.9, 129.0, 130.2, 138.6, 138.9, 140.3, 146.1, 151.2, 166.0, 166.0, 186.2; HRMS (ESI-TOF) m/z: $[M+Na]^+$ Calcd $C_{29}H_{24}N_2NaO_8S$ 583.1146, found 583.1138.

4.1.3. General Procedure for the Synthesis of 6-Alkylidene-γ-penicillanates

To a solution of tosylate salt **8** (1.00 g, 1.758 mmol) in dichloromethane (50 mL) a saturated aqueous solution of $NaHCO_3$ (50 mL) was added. The reaction mixture was stirred for 30 min at room temperature. The organic phase was separated, and the aqueous phase was extracted with dichloromethane. The combined organic extracts were dried with anhydrous Na_2SO_4 and concentrated under reduced pressure to obtain amino-γ-lactam **9** as a yellowish oil. To an ice-cold solution of freshly prepared amino-γ-lactam **9** in dichloromethane (100 mL), cold water (100 mL) was added followed by $HClO_4$ 1 M (3.8 mL) and $NaNO_2$ (0.32 mg, 4.40 mmol). The reaction mixture was stirred at 0 ºC for 1 h. The organic phase was separated off, and the aqueous phase was extracted with dichloromethane. The combined organic extracts were washed with cold saturated NaCl, dried (Na_2SO_4) and concentrated under reduced pressure (no heat) to give diazo-γ-lactam **10** as a yellow oil which was used without further purification. Rhodium acetate dimer (4×10^{-3} equiv., 7.0×10^{-3} mmol) was dissolved in toluene (25 mL) in a two-neck round bottom flask under inert atmosphere. Next, propylene oxide (99 equiv., 174 mmol, 13.8 mL) was added dropwise followed by a dropwise addition of a solution of the previously synthesized diazo-γ-lactam **10** in toluene (25 mL). The reaction mixture was stirred for 15 min and concentrated under reduced pressure. Benzhydryl 6-oxopenicillinate **11** was used without further purification. Benzhydryl 6-oxopenicillinate **11** was dissolved in dichloromethane (10 mL), the solution was cooled to –55 °C under nitrogen, and the appropriate phosphorus ylide (1.67 mmol) in dichloromethane (20 mL) was added dropwise. Stirring was continued for 15 min, then the solution was warmed to room

temperature and washed with water (20 mL). The organic layer was separated, dried (Na_2SO_4), and concentrated under reduced pressure.

4.1.3.1. (3S,7a,R,E)-benzhydryl 2,2-dimethyl-5-oxo-6-(2-oxo-2-phenylethylidene)hexahydropyrrolo[2,1-b]thiazole-3-carboxylate ***12a***

Prepared from 6-oxopenicillanate (1.758 mmol) and the corresponding phosphorus ylide (0.632 g, 1.67 mmol), as described in the general procedure. After purification by flash chromatography (hexane/ethyl acetate, 3:1), compound **12a** was obtained as a pale-yellow solid (246 mg, 0.494 mmol, 28%). mp 52.5–54.5 °C; $[\alpha]_D^{25}$ = + 220 (c 0.5 in CH_2Cl_2); IR (ATR) ν: 1169, 1254, 1364, 1448, 1496, 1670, 1702, 1738 and 2964 cm^{-1}; ^1H NMR δ ($CDCl_3$): 1.32 (s, 3H), 1.59 (s, 3H), 3.37 (dt, *J* = 21.0 and 2.9 Hz, 1H), 3.80 (ddd, *J* = 21.0, 6.9 and 2.8 Hz, 1H), 4.85 (s, 1H), 5.63 (dd, *J* = 6.9 and 2.5 Hz, 1H), 6.99 (s, 1H), 7.34-7.38 (m, 10H), 7.51 (t, *J* = 7.6 Hz, 2H), 7.61 (t, *J* = 7.4 Hz, 1H), 7.79 (t, *J* = 3.0 Hz, 2H), 8.02-8.04 (m, 2H); ^{13}C NMR δ ($CDCl_3$): 26.5, 31.8, 33.6, 59.5, 64.4, 68.6, 78.5, 123.1, 127.0, 127.8, 128.2, 128.4, 128.6, 128.6, 128.8, 133.6, 137.8, 139.2, 147.2, 167.4, 168.3, 190.4; HRMS (ESI-TOF) m/z: $[M+Na]^+$ Calcd $C_{30}H_{27}NNaO_4S$ 520.1553, found 520.1544.

4.1.3.2. (3S,7aR,E)-benzhydryl 2,2-dimethyl-5-oxo-6-(2-oxopropylidene)hexahydropyrrolo[2,1-b]thiazole-3-carboxylate ***12b***

Prepared from 6-oxopenicillanate (1.758 mmol) and the corresponding phosphorus ylide (0.531 g, 1.67 mmol), as described in the general procedure. After purification by flash chromatography (hexane/ethyl acetate, 3:1), compound **12b** was obtained as a white solid (121.1 mg, 0.278 mmol, 16%). mp 115.1–117.1 °C; $[\alpha]_D^{25}$ = + 250 (c 0.5 in CH_2Cl_2); IR (ATR) ν: 943, 966, 1155, 1169, 1216, 1269, 1357, 1401, 1492, 1637, 1686 and 1756 cm^{-1}; ^1H NMR δ ($CDCl_3$): 1.30 (s, 3H), 1.56 (s, 3H), 2.35 (s, 3H), 3.21 (dt, *J* = 21.1 and 2.9 Hz, 1H), 3.65 (ddd, *J* = 21.0, 6.9 and 2.8 Hz, 1H), 4.80 (s, 1H), 5.58 (dd, *J* = 6.9 and 2.6 Hz, 1H), 6.97 (s, 1H), 7.00 (t, *J* = 3.0 Hz, 1H), 7.30-7.36 (m, 10H); ^{13}C NMR δ ($CDCl_3$): 26.6, 31.9, 32.0, 33.4, 59.6, 64.4, 68.7, 78.7, 126.2, 127.1, 127.9, 128.3, 128.6, 128.7, 128.8, 139.3, 145.3, 167.5, 168.4, 198.5; HRMS (ESI-TOF) m/z: $[M+Na]^+$ Calcd $C_{25}H_{25}NNaO_4S$ 458.1397, found 458.1389.

4.1.3.3. (3S,7aR,E)-benzhydryl 6-(2-methoxy-2-oxoethylidene)-2,2-dimethyl-5-oxohexahydropyrrolo[2,1-b]thiazole-3-carboxylate ***12c***

Prepared from 6-oxopenicillanate (1.758 mmol) and the corresponding phosphorus ylide (0.558 g, 1.67 mmol), as described in the general procedure. After purification by flash chromatography (hexane/ethyl acetate, 3:1), compound **12c** was obtained as a yellow solid (219.3 mg, 0.485 mmol, 27%). mp 165.1–167.1 °C; $[\alpha]_D^{25}$ = + 220 (c 0.5 in CH_2Cl_2); IR (ATR) ν: 956, 1155, 1173, 1211, 1259, 1357, 1438, 1458, 1497, 1703, 1706 and 1745 cm^{-1}; ^1H NMR δ ($CDCl_3$): 1.30 (s, 3H), 1.56 (s, 3H), 3,21-3,28 (dt, *J* = 20.6 and 3.0 Hz, 1H), 3.63-3.71 (ddd, *J* = 20.6, 7.0 and 2.8 Hz, 1H), 3.79 (s, 3H), 4.81 (s, 1H), 5.59 (dd, *J* = 7.0 and 2.7 Hz, 1H), 6,68 (t, *J* = 3.0 Hz, 1H), 6,97 (s, 1H), 7.28-7.36 (m, 10H); ^{13}C NMR δ ($CDCl_3$): 26.6, 32.0, 33.0, 52.1, 60.0, 64.2, 68.7, 78.7, 121.4, 127.1, 127.9, 128.3, 128.6, 128.7, 128.8, 139.3, 147.6, 166.3, 167.5, 167.6 HRMS (ESI-TOF) m/z: $[M+Na]^+$ Calcd $C_{25}H_{25}NNaO_5S$ 474.1346, found 474.1338.

4.1.4. X-Ray diffraction studies

A crystal suitable for single-crystal X-ray analysis of compound **12c** was selected, covered with Fomblin (polyfluoro ether oil) and mounted on a nylon loop. The data were collected at room temperature on a Bruker APEX-II diffractometer equipped with a CCD detector, using graphite monochromated Mo-Kα radiation (λ=0.71073 Å). The data was processed using the APEX2 suite software package, which includes integration and scaling (SAINT), absorption corrections (SADABS)[17] and space group determination (XPREP). Structure solution and refinement were done using direct methods with the programs SIR2014[18] and SHELXL (version 2018/1)[19] inbuilt in APEX and WinGX-Version 2020.1[20] software packages. All non-hydrogen atoms were refined anisotropically. All hydrogen atoms were inserted in idealized positions and allowed to refine riding on the parent carbon or oxygen atom with C–H distances of 0.93 Å, 0.96 Å, and 0.97 Å and 0.98 Å, for aromatic, methyl, methylene and methine H atoms, respectively. The molecular diagrams were drawn with ORTEP3 (version 2020.1) included in the software package. Crystal data for **12c**: $C_{25}H_{25}NO_5S$, FW = 451.52, orthorhombic, space group $P2_12_12_1$ (no.19), D*c* = 1.310 gcm^{-3}, Z = 4, a = 7.711(2), b = 13.680(5), c = 21.707(8) Å, α = β = γ = 90 °, V = 2289.7(13) Å^3, T = 296(2) K, Bruker APEX-II diffractometer with CCD area detector, λ (MoKα) = 0.71073 Å, μ = 0.178 mm^{-1}. Of 12084 reflections measured, 4328 were unique. Refinement on F^2 concluded with the values R_1 = 0.0514 and wR_2 = 0.1001 for 292 parameters and 2630 data with I > 2σI. The data was deposited in CCDC under the deposit number 2129778.

Crystals suitable for single-crystal X-ray analysis of compounds **1i** and **12c** were selected, covered with Fomblin (polyfluoro ether oil) and mounted on a nylon loop. The data were collected at room temperature on a Bruker D8 Quest equipped with a Photon II detector (for **1i**) or on a Bruker APEX-II diffractometer equipped with a CCD detector (for **12c**), using graphite monochromated Mo-Kα radiation (λ=0.71073 Å). The data was processed using the APEX4 (**1i**) and APEX2 (**12c**) suite software package, which includes integration and scaling (SAINT), absorption corrections (SADABS)[17] and space group determination (XPREP). Structure solution and refinement were done using direct methods with the programs SIR2014,[18] SHELXT (version 2018/2) and SHELXL (version 2018/3)[19] inbuilt in APEX and WinGX-Version 2020.1[20] software packages. All non-hydrogen atoms were refined anisotropically. All hydrogen atoms were inserted in idealized positions and allowed to refine riding on the parent carbon or oxygen atom with C–H distances of 0.93 Å, 0.96 Å, and 0.97 Å and 0.98 Å, for aromatic, methyl, methylene and methine H atoms, respectively. The molecular diagrams were drawn with ORTEP3 (version 2021.3) included in the software package. Crystal data for **1i**: $C_{33}H_{27}NO_4S$, FW = 533.61, orthorhombic, space group $P2_12_12_1$ (no.19), D*c* = 1.292 gcm^{-3}, Z = 4, a = 6.2051(15), b = 15.066(4), c = 29.350(8) Å, α = β = γ = 90 °, V = 2289.7(13) Å^3, T = 296(2) K, Bruker D8 Quest diffractometer with Photon II detector, λ (MoKα) = 0.71073 Å, μ = 0.157 mm^{-1}. Of 51126 reflections measured, 5575 were unique. Refinement on F^2 concluded with the values R_1 = 0.0862 and wR_2 = 0.0969 for 354 parameters and 3581 data with I > 2σI. Crystal data for **12c**: $C_{25}H_{25}NO_5S$, FW = 451.52, orthorhombic, space group $P2_12_12_1$ (no.19), D*c* = 1.310 gcm^{-3}, Z = 4, a = 7.711(2), b = 13.680(5), c = 21.707(8) Å, α = β = γ = 90 °, V = 2289.7(13) Å^3, T = 296(2) K, Bruker APEX-II diffractometer with CCD area detector, λ (MoKα) = 0.71073 Å, μ = 0.178 mm^{-1}. Of 12084 reflections measured, 4328 were unique. Refinement on F^2 concluded with the values R_1 = 0.0514 and wR_2 = 0.1001 for 292 parameters and 2630 data with I > 2σI. The data were deposited in CCDC under the deposit numbers 2150367 for **1i** and 2129778 for **12c**.

4.2. Biological biology

Cell culture conditions: The A375 human melanoma cell line, the HT-1080 human fibrosarcoma cell line and the H1299 human lung cancer cell line were cultured in Dulbecco's Modified Eagle medium (DMEM, Sigma D-5648) supplemented with 10% heat-inactivated fetal bovine serum (FBS, Sigma F7524), 1% Penicillin-Streptomycin (100 U/mL penicillin and 10 µg/mL streptomycin, Gibco 15140-122) and 100 µM sodium pyruvate (Gibco Invitrogen Life Technologies; Gibco 1360). The OE19 esophageal carcinoma cell line was cultured in Roswell Park Memorial Institute 1640 medium (RPMI 1640, Sigma R4130), supplemented with 10% heat-inactivated fetal bovine serum (FBS, Sigma F7524), 1% penicillin-streptomycin (100 U/mL penicillin and 10 mg/mL streptomycin, Gibco 15140-122), and 400 mM sodium pyruvate (Gibco Invitrogen Life Technologies; Gibco 1360). All cell lines were kept at 37 °C, in a humidified incubator with 95% air and 5% CO_2. For all studies, cells were detached using a solution of 0.25% trypsin-EDTA (Gibco).

4.2.1. Cytotoxicity

The cells were plated in 48-well culture plates at a density of 1×10^5 cells per well and incubated overnight to allow cell attachment. Stock solutions at 10 mM of all compounds were prepared in dimethylsulphoxide (DMSO, Sigma Aldrich®, EUA). Cells were then incubated in the presence of serial-fold dilutions of the compounds for 48 or 72 h. Each dilution of each compound was performed in triplicate wells. Cell controls (cells without test compound), and vehicle controls (cells with 1% DMSO) were included in each assay. The metabolic activity was determined by MTT colorimetric assay (3-(4,5-dimethylthiazol-2-yl)-2,5-diphenyl tetrazolium bromide; MTT, Sigma Aldrich®, EUA). Briefly, cell cultures were washed with phosphate saline buffer (PBS: 137 mM NaCl, 2.7 mM KCl, 10 mM $Na_2HPO_4{\cdot}2H_2O$, 2.0 mM KH_2PO_4; pH = 7.4) and incubated with 0.5 mg mL^{-1} MTT (Sigma Aldrich®, EUA), pH = 7.4, at 37 °C for 4 h. Then, formazan crystals were dissolved in acid isopropanol (0.04 M 37% hydrochloric acid in isopropanol, Sigma Aldrich®, EUA). Absorbance was measured using an EnSpire Multimode Plate Reader (PerkinElmer). The results allowed to establish dose–response curves and to calculate IC_{50} values, the concentration required to inhibit cell proliferation by 50%.

4.2.2. Types of cell death

For types of cell death analysis, the cells were plated in 6-well culture plates at a density of 5×10^5 cells per well and incubated overnight to allow attachment and then were treated with compounds **1l**, **1m**, **1o** and **6a** at 5 and 10 µM. Then, cells were collected, centrifuged and washed with PBS prior to incubation with binding buffer, 2.5 µL An-V–FITC and 1 µL propidium iodide (kit Immunotech) for 15 min, at 4 °C in the dark. 400 µL PBS were added and samples were analyzed in a FACSCalibur cytometer (BD Biosciences, EUA). Excitation was set at 488 nm, and the emission filters were set at for An-V–FITC and propidium iodide, respectively.

4.2.3. Cellular Morphology

Morphological characteristics were evaluated by optical microscopy (Nikon Eclipse NI optical microscope, Nikon Instruments, Amsterdam, Netherlands) after staining with May-Grünwald Giemsa medium (Sigma 32856). The photographs were obtained from a

Nikon OS-Fi2 camera (Nikon Metrology Inc, Irvine, CA, USA) with magnifications of 50. The representative images of each condition were taken using the NIS-Elements D software (version 4.00).

4.2.4. Cell cycle analysis

For analysis of DNA content, 5×10^5 cells were incubated overnight to allow cell attachment and then were treated with compounds **1l**, **1m**, **1o** and **6a** at 5 and 10 μM. Cells were collected, centrifuged, and fixed with ice-cold ethanol (70%) for 30 min in the dark. Then, cells were washed with PBS and incubated with PI/RNase solution (Immunostep) for 15 min at rt. Cells were analyzed in the FACSCalibur cytometer with an excitation wavelength of 488 nm, and emission filter at of 585/42.

4.2.5. Production of reactive oxygen species

For analysis of reactive oxygen species, 5×10^5 cells were incubated overnight to allow cell attachment and then were treated with compounds **1l**, **1m**, **1o** and **6a** at 5 and 10 μM. Production of intracellular peroxides was determined by incubation of 5 μM of 2′,7′-dichlorodihydrofluorescein diacetate (DCFH2-DA, Invitrogen Life technologies, D399) probe, for 45 min in the dark at 37 °C. After washing, detection was performed with the excitation and emission wavelengths of 485 and 528 nm, respectively. The production of superoxide anion was evaluated using 2 μM dihydroethidium (DHE, Sigma D7008) probe, incubated during 10 min with the cells, at room temperature in the dark. Reading was performed using the excitation and emission wavelengths of 530 and 645 nm, respectively.

4.2.6. Gelatin Zymography

Total protein extracts were prepared on ice using a solution of radioimmuno precipitation assay (RIPA) buffer, and protein content was determined by bicinchoninic acid method (Pierce, 23250). Equal amounts of protein were incubated in Gelatin-containing polyacrylamide gels. 7.5% SDS-polyacrylamide separating gels with 4 mg/mL of gelatin (30% bis-acrylamide, 1.5 M tris-HCL pH 8.8, 10% ammonium persulfate, TEMED, 10% SDS and distilled water to reach final volume) and 5% SDS-polyacrylamide staking gels (30% bis-acrylamide, 0.5 M tris-HCL pH 6.8, 10% ammonium persulfate, TEMED, 10% SDS and distilled water to reach final volume) were prepared. The gels were loaded with samples diluted in 5x non-reducing buffer (25% 0.5 M Tris-HCl pH 6.8, 20% glycerol, 4% SDS, and 0.01% bromophenol blue) and the electrophoresis was carried using a constant electric potential of 90 V until satisfactory separation of interest bands. Gels were washed twice on washing buffer (2.5% Triton X-100, 5% 1 M Tris-HCl pH 7.5, 0.25% 2 M $CaCl_2$, 0.001% 0.1 M $ZnCl_2$) for 30 minutes, washed for 10 minutes on incubation buffer (1% Triton X-100, 5% 1 M Tris-HCl pH 7.5, 0.25% 2 M $CaCl_2$, 0.001% 0.1 M $ZnCl_2$) and incubated on incubation buffer for 24 hours at 37 ºC. The gels were stained by using Coomassie Blue staining solution (with 40% methanol and 10% acetic acid) for 0.5-1 h, and destained with a 40% methanol and 10% acetic acid solution. The active form of MMP-9 was visualized on gels. MMP-9 activity was quantified densitometrically with ImageJ software (http://imagej.nih.gov/ij/; provided in the public domain by the National Institutes of Health, Bethesda, MD, USA).

4.2.7. Statistical analysis

Statistical analysis was performed using Prism version 5.01 for Windows (GrahPad Software, San Diego, California USA, www.graphpad.com) with a level of significance of 5%. The 50% (IC_{50}) inhibitory concentrations, as well as the dose–response curve slopes, were estimated by plotting the percent metabolic activity (y axis) against the $\log_{10}$ concentration of each compound (x axis) and using the sigmoidal dose–response (variable slope) equation. The normality of the distribution of each quantitative variable was evaluated according to the Shapiro-Wilk test, with the aim of determining the use of parametric or non-parametric tests. The normalized values (superoxide anion, peroxides) of the experimental conditions were compared with the respective normalization value using the Kruskal-Wallis test with the correction of P value for multiple comparisons. The rest of the cellular studies (cell death and cell cycle) and zymography assays were compared with ANOVA test in cases where normal distribution and homogeneity of variances were verified or with the Kruskal-Wallis test with the correction of P value for multiple comparisons in the otherwise.

5. Declaration of competing interest

The authors declare that they have no known competing financial interests or personal relationships that could have appeared to influence the work reported in this paper.

6. Acknowledgements

The authors thank Coimbra Chemistry Centre (CQC), supported by the Portuguese Agency for Scientific Research, "Fundação para a Ciência e a Tecnologia" (FCT) through project UIDB/00313/2020 and UIDP/00313/2020, co-funded by COMPETE2020-UE. Acknowledgements are also due to CIBB, funded by FCT through projects UID/NEU/04539/2019, UIDB/04539/2020, UIDP/04539/2020, co-funded by COMPETE-FEDER (POCI-01-0145-FEDER-007440). The Associate Laboratory for Green Chemistry (LAQV), the Applied Molecular Biosciences Unit (UCIBIO), and the Associate Laboratory Institute for Health and Bioeconomy (i4HB) are financed by FCT (UIDB/50006/2020 and UIDP/50006/2020, LA/P/0008/2020, UIDB/04378/2020 and UIDP/04378/2020, and LA/P/0140/2020, respectively). X-ray infrastructure is financed by FCT-MCTES through project RECI/BBB-BEP/0124/2012. Américo J. S. Alves thanks FCT for fellowship SFRH/BD/128910/2017. The authors also acknowledge the UC-NMR facility for obtaining the NMR data (www.nmrccc.uc.pt).

7. Supplementary data

Supplementary data (copies of ^{1}H, ^{13}C NMR Spectra for New Compounds, IC_{50} data for 72 h incubation MTT assays and dose–response curves of MTT assays) associated with this article can be found, in the online version, at http://dx.doi.org/10.1016/j.bmc.xxxxx

8. References

[1] O. World Health, *WHO report on cancer: setting priorities, investing wisely and providing care for all*, World Health Organization, Geneva, **2020**.

[2] a) K. Bukowski, M. Kciuk and R. Kontek, *Int. J. Mol. Sci.* **2020**, *21*, 3233; b) Cancer multidrug resistance, *Nat. Biotechnol.* **2000**, *18*, IT18-IT20.

[3] a) N. Arya, A. Y. Jagdale, T. A. Patil, S. S. Yeramwar, S. S. Holikatti, J. Dwivedi, C. J. Shishoo and K. S. Jain, *Eur. J. Med. Chem.* **2014**, *74*, 619-656; b) P. D. Mehta, N. P. S. Sengar and A. K. Pathak, *Eur. J. Med. Chem.* **2010**, *45*, 5541-5560.

[4] a) P. Zhou, Y. Liu, L. Zhou, K. Zhu, K. Feng, H. Zhang, Y. Liang, H. Jiang, C. Luo, M. Liu and Y. Wang, *J. Med. Chem.* **2016**, *59*, 10329-10334; b) V. Blank, Y. Bellizzi, E. Zotta, P. G. Cornier, C. M. L. Delpiccolo, D. B. Boggián, E. G. Mata and L. P. Roguin, *Anticancer Drugs* **2018**, *29*; c) A. Banerjee, M. Dahiya, M. T. Anand and S. Kumar, *Asian Pac. J. Cancer Prev.* **2013**, *14*, 2127-2130; d) P. Pérez-Faginas, M. T. Aranda, M. T. García-López, A. Francesch, C. Cuevas and R. González-Muñiz, *Eur. J. Med. Chem.* **2011**, *46*, 5108-5119; e) A. M. Malebari, D. Fayne, S. M. Nathwani, F. O'Connell, S. Noorani, B. Twamley, N. M. O'Boyle, J. O'Sullivan, D. M. Zisterer and M. J. Meegan, *Eur. J. Med. Chem.* **2020**, *189*, 112050; f) M. Mohamadzadeh, M. Zarei and M. Vessal, *Bioorg. Chem.* **2020**, *95*, 103515; g) M. Mohamadzadeh and M. Zarei, *Mol. Divers.* **2020**, *25*, 2429-2439; h) N. Borazjani, M. Behzadi, M. Dadkhah Aseman, A. Jarrahpour, J. A. Rad, S. Kianpour, A. Iraji, S. M. Nabavizadeh, M. M. Ghanbari, G. Batta and E. Turos, *Med. Chem. Res.* **2020**, *29*, 1355-1375.

[5] a) S. Coe, N. Pereira, J. V. Geden, G. J. Clarkson, D. J. Fox, R. M. Napier, P. Neve and M. Shipman, *Org. Biomol. Chem.* **2015**, *13*, 7655-7663; b) B. S. Santos and T. M. V. D. Pinho e Melo, *Eur. J. Org. Chem.* **2013**, *2013*, 3901-3909; c) A. J. S. Alves and T. M. V. D. Pinho e Melo, *Eur. J. Org. Chem.* **2020**, *2020*, 6259-6269; d) H. Dao Thi, B. Danneels, T. Desmet, K. Van Hecke, T. Van Nguyen and M. D'hooghe, *Asian J. Org. Chem.* **2016**, *5*, 1480-1491; e) S. Li, W.-J. Cao and J.-A. Ma, *Synlett* **2017**, *28*, 673-678; f) H. Dao Thi, T. Van Nguyen and M. D'hooghe, *Monatsh. Chem.* **2018**, *149*, 687-700; g) Y. Kumar, P. M. S. Bedi, P. Singh, A. A. Adeniyi, A. Singh-Pillay, P. Singh and G. Bhargava, *ChemistrySelect* **2018**, *3*, 9484-9492; h) M. Humpl, J. Tauchman, N. Topolovčan, J. Kretschmer, F. Hessler, I. Císařová, M. Kotora and J. Veselý, *J. Org. Chem.* **2016**, *81*, 7692-7699; i) Y. Liang, R. Raju, T. Le, C. D. Taylor and A. R. Howell, *Tetrahedron Lett.* **2009**, *50*, 1020-1022; j) N. G. Alves, I. Bártolo, A. J. S. Alves, D. Fontinha, D. Francisco, S. M. M. Lopes, M. I. L. Soares, C. J. V. Simões, M. Prudêncio, N. Taveira and T. M. V. D. Pinho e Melo, *Eur. J. Med. Chem.* **2021**, *219*, 113439; k) S.-Q. Luo, W. Liu, B.-F. Ruan, S.-L. Fan, H.-X. Zhu, W. Tao and H. Xiao, *Org. Biomol. Chem.* **2020**, *18*, 4599-4603.

[6] a) G. Cainelli, P. Galletti, S. Garbisa, D. Giacomini, L. Sartor and A. Quintavalla, *Bioorg. Med. Chem.* **2003**, *11*, 5391-5399; b) G. Cainelli, P. Galletti, S. Garbisa, D. Giacomini, L. Sartor and A. Quintavalla, *Bioorg. Med. Chem.* **2005**, *13*, 6120-6132; c) D. Giacomini, R. Musumeci, P. Galletti, G. Martelli, L. Assennato, G. Sacchetti, A. Guerrini, E. Calaresu, M. Martinelli and C. Cocuzza, *Eur. J. Med. Chem.* **2017**, *140*, 604-614; d) G. Cainelli, C. Angeloni, R. Cervellati, P. Galletti, D. Giacomini, S. Hrelia and R. Sinisi, *Chem. Biodiversity* **2008**, *5*, 811-829; e) I. Dell'Aica, L. Sartor, P. Galletti, D. Giacomini, A. Quintavalla, F. Calabrese, C. Giacometti, E. Brunetta, F. Piazza, C. Agostini and S. Garbisa, *J. Pharmacol. Exp.*

Ther. **2006**, *316*, 539-546; f) E. A. Rodkey, D. C. McLeod, C. R. Bethel, K. M. Smith, Y. Xu, W. Chai, T. Che, P. R. Carey, R. A. Bonomo, F. van den Akker and J. D. Buynak, *J. Am. Chem. Soc.* **2013**, *135*, 18358-18369; g) G. Bou, E. Santillana, A. Sheri, A. Beceiro, J. M. Sampson, M. Kalp, C. R. Bethel, A. M. Distler, S. M. Drawz, S. R. R. Pagadala, F. van den Akker, R. A. Bonomo, A. Romero and J. D. Buynak, *J. Am. Chem. Soc.* **2010**, *132*, 13320-13331; h) J. D. Buynak, B. Geng, B. Bachmann and H. Ling, *Bioorganic Med. Chem. Lett.* **1995**, *5*, 1513-1518; i) B. Di Giacomo, G. Tarzia, A. Bedini, G. Gatti, F. Bartoccini, C. Balsamini, A. Tontini, W. Baffone, E. Di Modugno and A. Felici, *Farmaco* **2002**, *57*, 273-283; j) J. D. Buynak, A. S. Rao, G. P. Ford, C. Carver, G. Adam, B. Geng, B. Bachmann, S. Shobassy and S. Lackey, *J. Med. Chem.* **1997**, *40*, 3423-3433; k) J. D. Buynak, K. Wu, B. Bachmann, D. Khasnis, L. Hua, H. K. Nguyen and C. L. Carver, *J. Med. Chem.* **1995**, *38*, 1022-1034.

[7] a) G. Veinberg, M. Vorona, I. Shestakova, I. Kanepe, O. Zharkova, R. Mezapuke, I. Turovskis, I. Kalvinsh and E. Lukevics, *Bioorg. Med. Chem.* **2000**, *8*, 1033-1040; b) G. Veinberg, I. Shestakova, M. Vorona, I. Kanepe and E. Lukevics, *Bioorganic Med. Chem. Lett.* **2004**, *14*, 147-150; c) M. Vorona, I. Potorochina, G. Veinberg, S. Belyakov, I. Shestakova, I. Kanepe and E. Lukevics, *Chem. Heterocycl. Compd.* **2009**, *45*, 1532-1538.

[8] a) J. Caruano, G. G. Muccioli and R. Robiette, *Org. Biomol. Chem.* **2016**, *14*, 10134-10156; b) A. Albrecht, Ł. Albrecht and T. Janecki, *Eur. J. Org. Chem.* **2011**, *2011*, 2747-2766; c) A. Albrecht, Ł. Albrecht, M. Różalski, U. Krajewska, A. Janecka, K. Studzian and T. Janecki, *New J. Chem.* **2010**, *34*, 750-761; d) H. Krawczyk, Ł. Albrecht, J. Wojciechowski, W. M. Wolf, U. Krajewska and M. Różalski, *Tetrahedron* **2008**, *64*, 6307-6314; e) A. Albrecht, J. F. Koszuk, J. Modranka, M. Różalski, U. Krajewska, A. Janecka, K. Studzian and T. Janecki, *Bioorg. Med. Chem.* **2008**, *16*, 4872-4882; f) T. Janecki, E. Błaszczyk, K. Studzian, A. Janecka, U. Krajewska and M. Różalski, *J. Med. Chem.* **2005**, *48*, 3516-3521; g) A. Janecka, A. Wyrębska, K. Gach, J. Fichna and T. Janecki, *Drug Discov. Today* **2012**, *17*, 561-572; h) J. Modranka, R. Jakubowski, M. Różalski, U. Krajewska, A. Janecka, K. Gach, D. Pomorska and T. Janecki, *Eur. J. Med. Chem.* **2015**, *92*, 565-574.

[9] J. C. Sheehan and T. J. Commons, *J. Org. Chem.* **1978**, *43*, 2203-2208.

[10] J. D. Buynak, A. Srinivasa Rao and S. D. Nidamarthy, *Tetrahedron Lett.* **1998**, *39*, 4945-4946.

[11] A. J. S. Alves, N. G. Alves, C. C. Caratão, M. I. M. Esteves, D. Fontinha, I. Bártolo, M. I. L. Soares, S. M. M. Lopes, M. Prudêncio, N. Taveira and T. M. V. D. Pinho e Melo, *Curr. Top. Med. Chem.* **2020**, *20*, 140-152.

[12] C. R. Groom, I. J. Bruno, M. P. Lightfoot and S. C. Ward, *Acta Crystallogr., Sect. B: Struct. Sci., Cryst. Eng. Mater.* **2016**, *72*, 171-179.

[13] a) J. R. Valcourt, J. M. S. Lemons, E. M. Haley, M. Kojima, O. O. Demuren and H. A. Coller, *Cell Cycle* **2012**, *11*, 1680-1696; b) O. Marescal and I. M. Cheeseman, *Dev. Cell* **2020**, *55*, 259-271; c) A. Recasens and L. Munoz, *Trends Pharmacol. Sci.* **2019**, *40*, 128-141; d) I. B. Dias, H. R. Bouma and R. H. Henning, *Front. Physiol.* **2021**, *12*

[14] a) S. Mondal, N. Adhikari, S. Banerjee, S. A. Amin and T. Jha, *Eur. J. Med. Chem.* **2020**, *194*, 112260; b) A. Winer, S. Adams and P. Mignatti, *Mol. Cancer Ther.* **2018**, *17*, 1147.

[15] J. Cathcart, A. Pulkoski-Gross and J. Cao, *Genes Dis.* **2015**, *2*, 26-34.

[16] a) G. A. Rosenberg, *Lancet Neurol.* **2009**, *8*, 205-216; b) J. M. Wells, M. M. Parker, R. A. Oster, R. P. Bowler, M. T. Dransfield, S. P. Bhatt, M. H. Cho, V. Kim, J. L. Curtis, F. J. Martinez, R. Paine, 3rd, W. O'Neal, W. W. Labaki, R. J. Kaner, I. Barjaktarevic, M. K. Han, E. K. Silverman, J. D. Crapo, R. G. Barr, P. Woodruff, P. J. Castaldi, A. Gaggar, Spiromics and C. O. Investigators, *JCI Insight* **2018**, *3*, e123614; c) M. Xue, K. McKelvey, K. Shen, N. Minhas, L. March, S.-Y. Park and C. J. Jackson, *Rheumatology* **2014**, *53*, 2270-2279; d) D. P. C. de Rooy, A. Zhernakova, R. Tsonaka, A. Willemze, B. A. S. Kurreeman, G. Trynka, L. van Toorn, R. E. M. Toes, T. W. J. Huizinga, J. J. Houwing-Duistermaat, P. K. Gregersen and A. H. M. van der Helm-van Mil, *Ann. Rheum. Dis.* **2014**, *73*, 1163; e) M. Ram, Y. Sherer and Y. Shoenfeld, *J. Clin. Immunol.* **2006**, *26*, 299-307; f) Z. Rahimi, Z. Abdan, Z. Rahimi, N. Razazian, H. Shiri, A. Vaisi-Raygani, E. Shakiba, M. Vessal and M.-T. Moradi, *Immunol. Invest.* **2016**, *45*, 543-552; g) A. Yabluchanskiy, Y. Ma, R. P. Iyer, M. E. Hall and M. L. Lindsey, *Physiology* **2013**, *28*, 391-403.

[17] L. Krause, R. Herbst-Irmer, G. M. Sheldrick and D. Stalke, *J. Appl. Crystallogr.* **2015**, *48*, 3-10.

[18] M. C. Burla, R. Caliandro, B. Carrozzini, G. L. Cascarano, C. Cuocci, C. Giacovazzo, M. Mallamo, A. Mazzone and G. Polidori, *J. Appl. Crystallogr.* **2015**, *48*, 306-309.

[19] a) G. Sheldrick, *Acta Cryst. C* **2015**, *71*, 3-8; b) C. B. Hubschle, G. M. Sheldrick and B. Dittrich, *J. Appl. Crystallogr.* **2011**, *44*, 1281-1284.

[20] L. Farrugia, *J. Appl. Crystallogr.* **2012**, *45*, 849-854.